Redox-Active Ferrocenyl Dendrimers: Thermodynamics and Kinetics of Adsorption, In-Situ Electrochemical Quartz Crystal Microbalance Study of the Redox Process and Tapping Mode AFM Imaging

Kazutake Takada,[†] Diego J. Díaz,[†] Héctor D. Abruña,*[,†] Isabel Cuadrado,*[,‡] Carmen Casado,[‡] Beatriz Alonso,[‡] Moisés Morán,*[,‡] and José Losada[‡]

Contribution from the Department of Chemistry, Baker Laboratory, Cornell University, Ithaca, New York, 14853-1301, and Departamento de Química Inorgánica, Universidad Autónoma de Madrid, Cantoblanco 28049, Madrid, Spain

Received May 19, 1997[⊗]

Abstract: The thermodynamics and kinetics of adsorption of the redox-active dendrimers diaminobutane-*dend*-$(NHCOFc)_8$, (dendrimer-Fc_8), diaminobutane-*dend*-$(NHCOFc)_{16}$, (dendrimer-Fc_{16}), diaminobutane-*dend*-$(NHCOFc)_{32}$, (dendrimer-Fc_{32}), and diaminobutane-*dend*-$(NHCOFc)_{64}$, (dendrimer-Fc_{64}) containing 8, 16, 32, and 64 ferrocenyl moieties on the periphery, respectively, have been studied using electrochemical and electrochemical quartz crystal microbalance (EQCM) techniques. All of these materials adsorb onto a Pt electrode surface. At an applied potential of 0.0 V (vs SSCE), where the ferrocenyl sites are in the reduced form and the dendrimers are neutral, the adsorption thermodynamics are well-characterized by the Langmuir adsorption isotherm. The kinetics of adsorption were activation-controlled and the rate constant decreased with decreasing size of the dendrimer. Potential scanning past +0.60 V, where the ferrocenyl sites are oxidized, gave rise to the electrodeposition of multilayer equivalents of the dendrimers. The additional material gradually desorbed upon rereduction, so only a monolayer equivalent remained on the electrode surface. Impedance analysis of the resonator response suggests that at multilayer equivalent coverages, the adsorbed dendrimers do not behave as rigid films and that incorporation of significant amounts of solvent and/or salt accompany the adsorption of these materials at such high coverages. On the other hand, at monolayer coverages, the adsorbed films appear to exhibit rigid film behavior. Using tapping mode atomic force microscopy we have been able to image dendrimer-Fc_{64} adsorbed onto a Pt(111) surface. The images reveal that the apparent size of the dendrimer adsorbed on the surface is significantly larger than estimated values based on calculations, which is ascribed to a flattening of the dendrimer upon adsorption.

Introduction

Recently the study of dendrimers has received a great deal of attention due to their highly ordered and branched molecular structures and their well-defined number of functional groups.[1] Novel dendrimers capable of exhibiting redox activity, containing redox-active units at the core, within the branches, or at the periphery of the dendritic structure have been recently prepared. In particular, the electrochemical behavior of redox-active metallodendrimers containing iron,[2−9] osmium, ruthenium,[10,11] and zinc[12] metal sites has been reported. The properties of such dendrimers are of great interest because the number of electrochemically active functional groups can be precisely controlled. Thus, by modifying an electrode surface with such dendrimers, it is possible to relate the number of electroactive species to their electrochemical properties. This may help provide important insights to the understanding of the mechanisms of interfacial reactions between an electrode and such highly branched and organized redox-active species. In addition, dendrimers modified with electrochemically active groups represent excellent candidates for use in practical applications such as catalysts, electron transfer mediators, ion sensors, or in electronic devices. Indeed, an application of ferrocenyl amido-based dendrimers as anion sensors has been recently reported.[8]

[†] Cornell University.

[‡] Universidad Autónoma de Madrid.

[⊗] Abstract published in *Advance ACS Abstracts,* October 15, 1997.

(1) For recent reviews on dendrimers, see: (a) Newkome, G. R.; Moorefield, C. N.; Vögtle, F. *Dendritic Molecules: Concepts, Synthesis, Perspectives*, VCH: Weinheim, 1996. (b) Newkome G. R., *Advances in Dendritic Macromolecules*; JAI Press: Greenwich, CT, 1994; Vol 1 and 1995; Vol 2. (c) Ardoin, N.; Astruc, D. *Bull. Soc. Chim. Fr.* **1995**, *132*, 875. (d) Issberner, J.; Moors, R.; Vögtle, F. *Angew. Chem., Int. Ed. Engl.* **1994**, *33*, 2413. (e) Fréchet, J. M. *Science* **1994**, *263*, 1710. (f) Tomalia, D. A.; Durst, H. D. In *Topics in Current Chemistry*; Weber, E., Ed.; Springer-Verlag: Berlin, 1993; Vol 165, p 193.

(2) Cuadrado, I.; Morán, M.; Losada, J.; Casado, C. M.; Pascual, C.; Alonso, B.; Lobete, F. In *Advances in Dendritic Macromolecules*; Newkome, G. R., Ed.; JAI Press: Greenwich, CT, 1996; Vol. 3, p 151.

(3) Cuadrado, I.; Morán, M.; Casado, C. M.; Alonso, B.; Lobete, F.; García, B.; Ibisate, M.; Losada, J. *Organometallics* **1996**, *15*, 5278.

(4) (a) Alonso, B.; Cuadrado, I.; Morán, M.; Losada, J. *J. Chem. Soc., Chem. Commun.* **1994**, 2575. (b) Alonso, B; Morán, M.; Casado, C. M.; Lobete, F.; Losada, J.; Cuadrado, I. *Chem. Mater.* **1995**, *7*, 1440. (c) Losada, J.; Cuadrado, I.; Morán, M.; Casado, C. M.; Alonso, B.; Barranco, M. *Anal. Chim. Acta* **1996**, *251*, 5.

(5) Fillaut, J.-L.; Linares, J.; Astruc, D. *Angew. Chem., Int. Ed. Engl.* **1994**, *33*, 2460.

(6) Chow, H.-F.; Chan, Y. Y.-K.; Chan, D. T. W.; Kwok, R. W. M. *Chem. Eur. J.* **1996**, *2*, 1085.

(7) Gorman, C. B.; Parkhurst, B. L.; Su, W. Y.; Chen, K.-Y. *J. Am. Chem. Soc.* **1997**, *119*, 1141.

(8) Valério, C.; Fillaut, J. -L.; Ruiz, J.; Guittard, J.; Blais, J.-C.; Astruc, D. *J. Am. Chem. Soc.* **1997**, *119*, 2588.

(9) Shu, C.-F.; Shen, H.-M. *J. Mater. Chem.* **1997**, *7*, 47.

(10) Newkome, G. R.; Güther, R.; Moorefield, C. N.; Cardullo, F.; Echegoyen, L.; Pérez-Cordero E.; Luftmann, H. *Angew. Chem. Int. Ed. Engl.* **1995**, *34*, 2023.

(11) Campagna, S.; Denti, G.; Serroni, S.; Juris, A.; Venturi, M.; Ricevuto, V.; Balzani, V. *Chem. Eur. J.* **1995**, *1*, 211.

(12) Dandliker, P. J.; Diederich, F.; Gross, M.; Knobler, C. B.; Louati, A.; Sanford, E. M. *Angew. Chem., Int. Ed. Engl.* **1994**, *33*, 1739.

S0002-7863(97)01631-4 CCC: $14.00

In this context, we have previously demonstrated that Pt and Au electrode surfaces can be modified with ferrocenyl silicon-based dendrimers and that the resulting films exhibit a well-defined redox response ascribed to the surface-immobilized ferrocenyl groups.[2,4] Shu et al. have recently reported on the synthesis and electrochemical properties of ferrocenyl aryl ether-based dendrimers. They have also demonstrated deposition of the ferrocenyl aryl ether-based dendrimers onto Pt electrodes.[9] It is clear that redox-active dendrimers represent a very attractive class of electrode modifiers with numerous potential applications such as that mentioned above.

We recently reported on the synthesis and electrochemistry of several diaminobutane-based poly(propylene imine) dendrimers functionalized at the periphery with 4, 8 (Figure 1A), 16, 32 (Figure 1B), or 64 (Figure 1C) ferrocenyl moieties, DAB-*dend*-$(NHCOFc)_x$ ($x = 4$, 8, 16, 32, and 64) (hereafter, referred to as dendrimers-Fc_x, $x = 4$, 8, 16, 32, and 64, respectively), and have demonstrated that these dendrimers show a well-defined, simultaneous multielectron transfer at the same potential in methylene chloride (CH_2Cl_2) solution.[3] In that study, we also reported that Pt electrodes could be modified with such dendrimers.

In this paper, we report on the adsorption thermodynamics and kinetics of these materials with emphasis on dendrimers-Fc_x ($x = 8$, 32, and 64) onto a Pt electrode by means of cyclic voltammetry. We have also investigated, in detail, the electroadsorption processes of dendrimers-Fc_x ($x = 8$, 16, 32, and 64) during potential cycling by means of the electrochemical quartz crystal microbalance (EQCM) and admittance measurements of the quartz crystal resonator on the basis of the electrical equivalent circuit analysis in CH_2Cl_2 solution. The electrochemical properties of Pt electrodes modified with dendrimers-Fc_x ($x = 8$, 16, 32, and 64) in acetonitrile (AN) were studied using the EQCM method, and changes in the film properties of these dendrimers during the redox processes were investigated by admittance measurements of the resonator.

Using tapping mode atomic force microscopy (TMAFM) we have been able to image dendrimer-Fc_{64} adsorbed onto a Pt-(111) electrode. The images reveal that the apparent size of the dendrimer adsorbed on the Pt electrode surface is significantly larger than values estimated on the basis of calculations.

Experimental Section

Materials. The dendritic polyamines DAB-*dend*-$(NH_2)_x$ ($x = 8$, 16, 32, and 64) were purchased from DSM. 1-Chlorocarbonylferrocene was prepared by treatment of ferrocenecarboxylic acid (Aldrich) with PCl_5.[13] CH_2Cl_2 and AN were purchased from Burdick and Jackson (distilled in glass) and dried over 4 Å molecular sieves prior to use. Tetra-*n*-butylammonium perchlorate (TBAP) (G. F. S. Chemicals) was recrystallized three times from ethyl acetate and dried under vacuum for 96 h. All other reagents (analytical grade) were used without further purification.

Apparatus. AT-cut quartz crystals (5 MHz) of 24.5 mm diameter with Pt electrodes deposited over a Ti adhesion layer (Maxtek) were used for EQCM measurements. An asymmetric keyhole electrode arrangement was used, in which the circular electrodes' geometrical areas were 1.370 cm^2 (front side) and 0.317 cm^2 (back side), respectively. The electrode surfaces were overtone polished. The quartz crystal resonator was set in a probe (TPS-550, Maxtek) made of Teflon, in which the oscillator circuit was included, and the quartz crystal was held vertically. The probe was connected to a conventional three-chamber electrochemical cell by a homemade Teflon joint. One of the electrodes of the quartz crystal resonator, in contact with the solution, was also used as the working electrode. The potential of the working electrode was controlled with a Bio-Analytical Systems (BAS) CV-27 potentiostat. A sodium chloride saturated calomel electrode (SSCE) and a coiled Pt wire were used as reference and counter electrodes, respectively, unless otherwise noted. The frequency response measured with a plating monitor (PM-740, Maxtek) and the current measured with the potentiostat were simultaneously recorded by a personal computer which was interfaced to the above instruments using LabVIEW (National Instruments). A Pt disk sealed in soft glass was used as a working electrode for conventional cyclic voltammetry, and the voltammograms were recorded on an Soltec X-Y recorder. The admittance of the quartz crystal resonator was measured near its resonant frequency by an impedance analyzer (HP4194A, Hewlett-Packard) equipped with a test lead (HP16048A). A probe similar to the one used in the EQCM measurements, but which did not include an oscillator circuit inside, was used to accomplish a direct connection between the quartz crystal resonator and the impedance analyzer.

TMAFM studies were carried out on a Nanoscope III (Digital Instruments), using a 12 μm, D scanner in air. The AFM was mounted on a homemade antivibration table and on an isolation chamber. AFM tips from Digital Instruments with force constants of 50 N/m (manufacturer's specifications) were employed. A resonant frequency of 270 kHz was used in the studies where tapping mode was employed.

The diameters of the various dendrimers were calculated using CACHe molecular mechanics calculations using a trans conformation about the amide bonds.

Synthesis of Ferrocenyl Dendrimers. All dendrimers were prepared following the same procedure. A mixture of the dendritic polyamine DAB-*dend*-$(NH_2)_x$ ($x = 8$, 16, 32, and 64), and triethylamine in CH_2Cl_2 was added dropwise to a stirred CH_2Cl_2 solution of the corresponding equivalents of 1-chlorocarbonylferrocene, under argon at room temperature. The condensation reactions were complete within a few minutes, as indicated by the solution IR spectrum of the reaction mixture which showed the disappearance of the band at 1754 cm^{-1} due to the starting C(O)Cl group and the appearance of new absorbances near 1635 and 1535 cm^{-1} corresponding to the formation of the amide group. The resulting solution was washed with saturated aqueous $NaHCO_3$ solution and brine, to remove the triethylamine hydrochloride byproduct, and dried over $MgSO_4$. After the removal of the solvent the products were purified by repeated reprecipitations from CH_2Cl_2/hexane. All organometallic dendrimers were isolated in high yields (95−98%) as air-stable orange solids, soluble in solvents such as CH_2Cl_2, tetrahydrofuran, and dimethylformide, but insoluble in AN and *n*-hexane. Microanalytical data for dendrimer-Fc_{32} and dendrimer-Fc_{64} are not included because of *n*-hexane inclusion in the inner dendritic cavities, as detected by ^1H NMR spectroscopy.[3]

Selected Spectroscopic and Analytical Data for Dendrimers. Dendrimer-Fc_8. ^1H NMR ($CDCl_3$): δ 7.32 (t, 8H, N*H*), 4.93 (t, 16H, C_5H_4), 4.34 (t, 16H, C_5H_4), 4.22 (s, 40H, Cp), 3.42 (br, 16H, $NHCH_2$), 2.46 (br, 36H, CH_2NCH_2), 1.74 (br, 28H,CH_2CH_2N), 1.43 (br, 4H, $NCH_2CH_2CH_2CH_2N$). $^{13}C\{^1H\}$ NMR ($CDCl_3$): δ 170.70 (*C*O), 70.38 (C_5H_4), 69.72 (Cp), 68.43 (C_5H_4), 51.78 (CH_2NCH_2), 38.15 (NH-CH_2), 27.16 ($CH_2CH_2CH_2$). MS (FAB; *m/z*): 2471 (M^+, $C_{128}H_{160}Fe_8O_8N_{14}$), calcd 2469. IR (KBr): amide I (ν(CO)) 1630 cm^{-1}, amide II (ν(CN),-1540 cm^{-1}. Anal. Calcd for $C_{128}H_{160}N_{14}Fe_8O_8$: C, 62.25; H, 6.53; N, 7.94. Found: C, 62.03; H, 6.47; N, 7.87.

Dendrimer-Fc_{16}. ^1H NMR ($CDCl_3$): δ 7.48 (t, 16H, N*H*), 4.93 (t, 32H, C_5H_4), 4.34 (t, 32H, C_5H_4), 4.22 (s, 80H, Cp), 3.45 (br, 32H, $NHCH_2$), 2.47 and 2.38 (br, 84H, CH_2NCH_2), 1.75 (m, 56H, CH_2CH_2-CH_2), 1.43 (br, 4H, $NCH_2CH_2CH_2CH_2N$). $^{13}C\{^1H\}$ NMR ($CDCl_3$): δ 170.61 (*C*O), 70.32 and 68.46 (C_5H_4), 69.71 (Cp), 52.48 and 51.80 (CH_2NCH_2), 38.75 (NH-CH_2), 27.31 ($CH_2CH_2CH_2$). MS (MALDI-TOF; *m/z* (%)): 5180 ($M + Ag^+$, 100); IR (KBr): amide I 1629 cm^{-1}, amide II 1539 cm^{-1}. Anal. Calcd. for $C_{264}H_{336}N_{30}Fe_{16}O_{16}$: C, 62.44; H, 6.62; N, 8.27. Found: C, 62.27; H, 6.74; N, 8.16.

Dendrimer-Fc_{32}. ^1H NMR ($CDCl_3$): δ 7.66 (t, 32H, N*H*), 4.97 (t, 64H, C_5H_4), 4.34 (t, 64H, C_5H_4), 4.22 (s, 160H, Cp), 3.44 (br, 64H, $NHCH_2$), 2.46 and 2.37 (br, 180H, CH_2NCH_2), 1.75 (br, 60H, CH_2CH_2-CH_2), 1.43 (br, 4H, $NCH_2CH_2CH_2CH_2N$). $^{13}C\{^1H\}$ NMR ($CDCl_3$): δ 170.71 (*C*O), 70.34 and 68.53 (C_5H_4), 69.73 (Cp), 52.47 and 51.79 (CH_2NCH_2), 38.34 (NH-CH_2), 27.33 ($CH_2CH_2CH_2$). MS (MALDI-TOF; *m/z*): 10290 (M^+, C536H$_{688}$N62Fe$_{32}$O$_{32}$), calcd 10295. IR (KBr): amide I 1631 cm^{-1}, amide II 1539 cm^{-1}.

Dendrimer-Fc_{64}. ^1H NMR ($CDCl_3$): δ 7.86 (br, 64H, N*H*), 5.00 (br, 128H, C_5H_4), 4.33 (br, 128H, C_5H_4), 4.21 (s, 320H, Cp), 3.43

(13) Pauson, P. L.; Watts, W. E. *J. Chem. Soc.* **1963**, 2990.

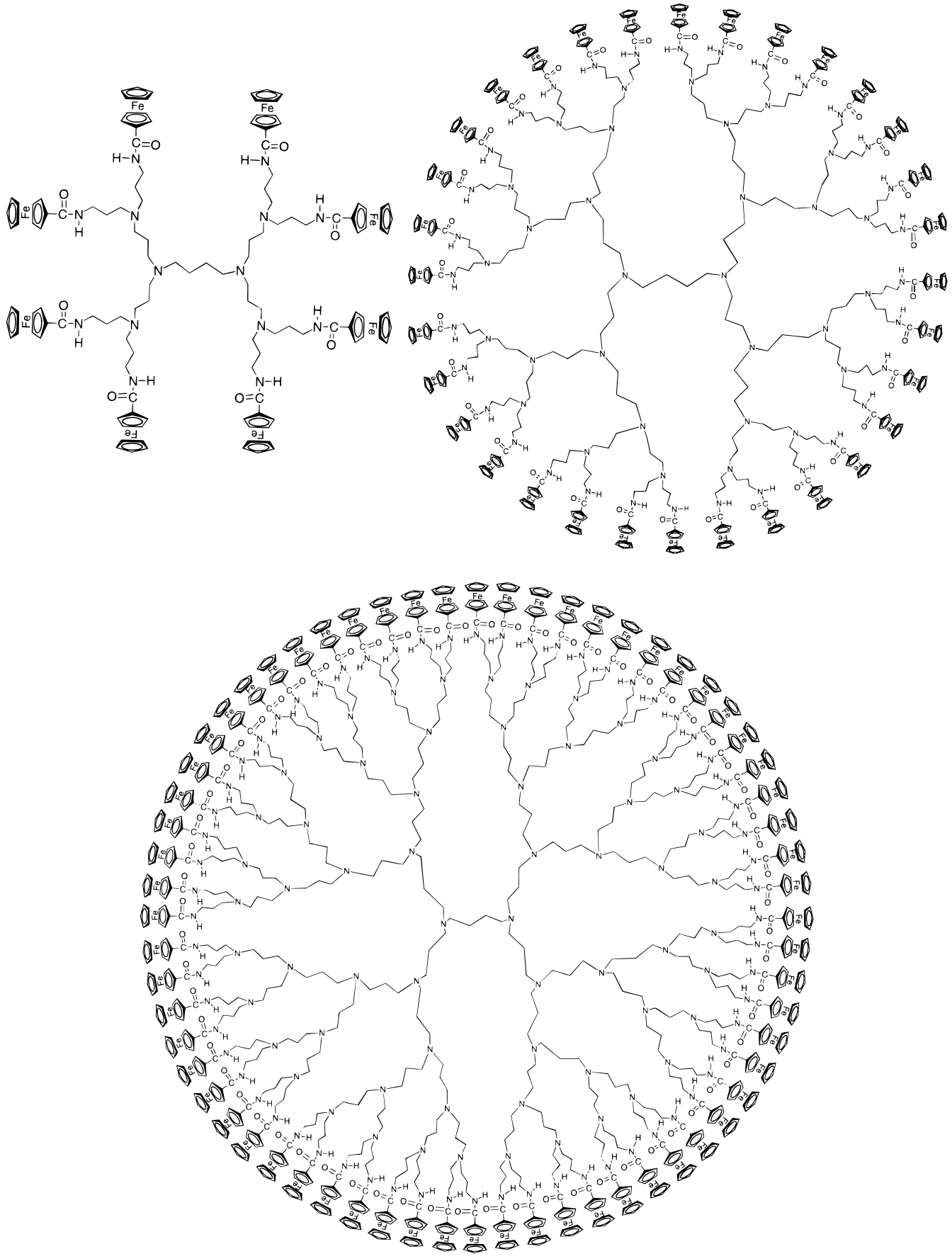

Figure 1. Structures of (A) diaminobutane-*dend*-$(NHCOFc)_8$ (dendrimer-Fc_8), (B) diaminobutane-*dend*-$(NHCOFc)_{32}$ (dendrimer-Fc_{32}), and (C) diaminobutane-*dend*-$(NHCOFc)_{64}$ (dendrimer-Fc_{64}).

(br, 128H, $NHCH_2$), 2.35 (br, 372H, CH_2NCH_2), 1.75 and 1.56 (br, 252H, CH_2CH_2N). $^{13}C\{^1H\}$ NMR ($CDCl_3$): δ 170.78 (*C*O), 70.39 and 68.60 (C_5H_4), 69.75 (Cp), 51.70 (CH_2NCH_2), 38.28 (NH-CH_2), 27.35 ($CH_2CH_2CH_2$). MS (MALDI-TOF; *m/z*): 20031 (broad, M^+,

$C_{1080}H_{1392}N_{126}Fe_{64}O_{64}$), calcd 20730. MS (MALDI-TOF, *m/z*) of the starting dendritic polyamine, DAB-*dend*-$(NH_2)_{64}$: 6926 (broad, M^+, $C_{376}H_{880}N_{126}$), calcd 7163. IR (KBr): amide I 1628 cm^{-1}, amide II 1537 cm^{-1}.

Procedures. For EQCM measurements the electrode was pretreated by continuous cycling between −0.20 and +1.20 V vs Ag/AgCl in a 0.1 M H_2SO_4 solution until the voltammetry of a clean polycrystalline platinum electrode was obtained. The electrode was subsequently rinsed with water and acetone and dried in air for 30 min. EQCM or admittance measurements of the quartz crystal resonator were carried out in a 0.10 M TBAP CH_2Cl_2 solution containing dendrimer-Fc_x (x = 8, 16, 32, or 64). After these measurements, the electrode was washed with CH_2Cl_2 and AN and placed in a clean cell containing a 0.10 M TBAP AN solution, and then EQCM or admittance experiments were carried out.

In the determination of adsorption data, the Pt disk electrode was prepared as above, except that it was polished with 1 μm diamond paste (Buehler) prior to use. The electrode was immersed in a 0.10 M TBAP CH_2Cl_2 solution and scanned between 0.0 V and +0.90 V vs SSCE until a steady voltammogram was obtained. The dendrimer was injected as a CH_2Cl_2 solution and the solution was homogenized by purging with nitrogen gas. The volume injected varied according to the desired final concentration of the dendrimer. The surface coverages were calculated from the integration of the cyclic voltammetric peaks (charge) associated with the ferrocene redox centers. Since the solution concentrations of the dendrimers were in the micromolar regime, their contribution to the measured current (charge) was negligible.[14] Therefore, the measured current (charge) arises only from the surface-confined species, and thus, surface coverage measurements can be carried out in the deposition solution with minimal error. The surface coverage was monitored as a function of time for all the dendrimers at different concentrations at 0.0 V vs SSCE. Nitrogen gas, passed through hydrocarbon and oxygen traps, was used to degas the solutions before use and flowed over the solutions during all experiments except during the acquisition of adsorption data in order to avoid changes in concentration due to evaporation of CH_2Cl_2.

TMAFM in air was employed in order to overcome difficulties in stability of the images found when using other imaging modes (e.g. STM and AFM) where the dendrimers were dragged by the tip. Tapping mode analysis was carried out at using a 12 μm (D) scanner. All TMAFM studies were carried out on a Pt(111) single crystal electrode modified with dendrimer-Fc_{64}.

The modified Pt samples for TMAFM analysis were prepared by immersion of a freshly flame-annealed Pt(111) single crystal (5.0 mm diameter and 2.5 mm in thickness) in a 0.052 mM dendrimer-Fc_{64} in CH_2Cl_2 solution for 2 h. The electrode was subsequently washed with fresh CH_2Cl_2 and air-dried before TMAFM analysis.

Tapping mode analysis was carried out at different size ranges from nanometers to microns at various locations on the surface prior to and after modification with dendrimer-Fc_{64}. All data were recorded in height mode. Setpoint values were chosen so that the interaction of the tip and the sample provided a good compromise between stability and resolution, without damaging the tip or the sample. Pushing the tip too close can damage the tip and can also accentuate the dragging of the dendrimer molecules by the tip. Keeping the tip too far typically results in a loss of resolution. Scan rates ranged from 1 to 3 Hz to avoid deformation of the image. At higher scan rates several problems arose ranging from damage of the tip to distortion of the image due to a slow vertical response for the surface profile. Images were taken at a 512 × 512 pixel resolution to increase the detail in the images.

Results and Discussion

1. Adsorption Process: A. Thermodynamics. Monolayer formation by self-assembly can be considered as the competition of ions, solvent, and adsorbate molecules in solution for binding sites on the surface of a substrate. Such a situation can be expressed as

$$A_{(sol)} + S_{(ads)} = A_{(ads)} + S_{(sol)} \quad (1)$$

where $A_{(sol)}$ represents adsorbate molecules in solution, $S_{(ads)}$ is the solvent and/or ions adsorbed on the substrate, $A_{(ads)}$ represents the molecules adsorbed on the substrate, and $S_{(sol)}$ is the solvent and/or ions displaced into the solution by the adsorbate. The amount of material adsorbed on the substrate (coverage) will depend on the concentration of the adsorbate in solution, $A_{(sol)}$. At low concentrations of $A_{(sol)}$, a fraction of a monolayer will be formed. As the solution concentration increases, so does the coverage, until a concentration value is reached at which the substrate's surface is saturated. At concentrations above this value, a saturation coverage is always obtained. The equilibrium relationship between the bulk solution concentration C^* and coverage Γ of adsorbate molecules is represented by an adsorption isotherm. Several types of isotherms have been proposed[16] and the differences among them depend on the type of adsorbate-adsorbate interactions allowed. The simplest adsorption isotherm is the Langmuir isotherm, which describes the adsorption process when the only adsorbate interaction is due to size, assuming that no other interactions are present. The Langmuir isotherm can be expressed as

$$\beta C^* = \frac{\theta}{1-\theta} \quad (2)$$

where β is the adsorption coefficient, C^* is the solution concentration of A ($A_{(sol)}$), and θ is the fractional coverage defined as Γ/Γ_s, where Γ_s is the saturation surface coverage.

If interactions such as attraction or repulsion between adsorbates are taken into account, an exponential term is added to the Langmuir adsorption isotherm. One of the simpler isotherms that takes into account such interactions is the Frumkin adsorption isotherm.[16]

$$\beta C^* = \frac{\theta}{1-\theta}\exp(-2a\theta) \quad (3)$$

where a represents an interaction parameter. When no interactions exist between adsorbates, this equation reduces to the Langmuir isotherm (eq 2), while positive and negative values of a indicate repulsive and attractive interactions, respectively.

In the present report, the adsorption thermodynamics of the dendrimers-Fc_x were studied using cyclic voltammetry to determine the surface coverage. Figure 2 shows a typical cyclic voltammogram of a Pt electrode modified with the dendrimer-Fc_{64} in a 0.10 M TBAP CH_2Cl_2 solution containing 93.8 nM dendrimer-Fc_{64} (= 6.0 μM ferrocene sites). Similar cyclic voltammograms were obtained for a variety of concentrations as well as for all the different dendrimers-Fc_x examined. Analogous cyclic voltammograms have been previously reported for ferrocenyl-containing silicon dendrimers.[4b] As can be seen in Figure 2, the cyclic voltammogram (from 0 to +1.0 V) exhibits a single peak with the symmetrical wave shape anticipated for a surface immobilized redox couple. The fact that only a single redox process is observed, implies a simultaneous multielectron transfer of all the ferrocene centers at the same potential. In addition the full width at half-maximum (ΔE_{FWHM}) of the voltammetric wave suggests that there are no significant near neighbor interactions present between the ferrocene groups. This behavior contrasts that often exhibited by multilayer equivalent films of poly(vinylferrocene),[15] which can be used as a point of comparison.

(14) (a) Acevedo, D.; Abruña, H. D. *J. Phys. Chem.* **1991**, *95*, 9590. (b) Tirado, J. D.; Acevedo, D.; Bretz, R. L.; Abruña, H. D. *Langmuir* **1994**, *10*, 1971.

(15) Peerce, P. J.; Bard, A. J. *J. Electroanal. Chem.* **1980**, *114*, 89.

(16) Trasatti, S. *J. Electroanal. Chem.* **1974**, *53*, 335.

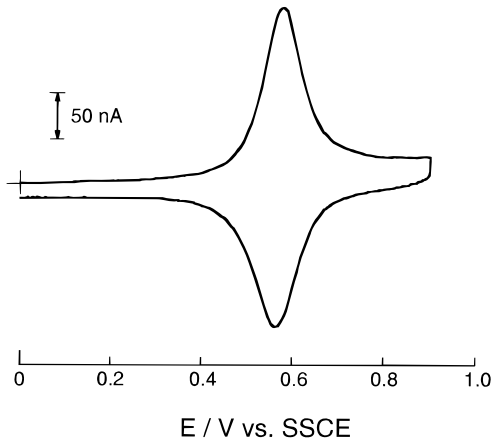

Figure 2. Cyclic voltammogram of a Pt electrode modified with a film of dendrimer-Fc_{64} adsorbed from a 0.10 M TBAP CH_2Cl_2 solution containing 93.8 nM dendrimer-Fc_{64} (= 6.0 μM Ferrocene sites). Scan rate is 100 mV s^{-1}.

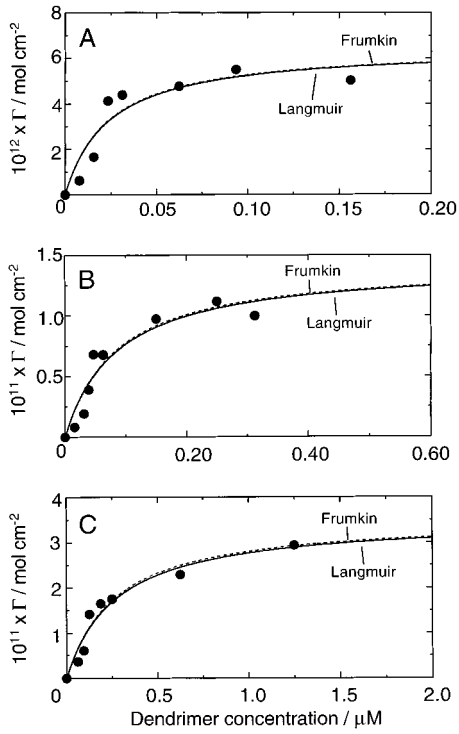

Figure 3. Langmuir (solid line) and Frumkin (broken line) isotherms fitted to experimental points for (A) dendrimer-Fc_{64}, (B) dendrimer-Fc_{32}, and (C) dendrimer-Fc_8 adsorbed to a Pt electrode at 0.0 V vs SSCE in a 0.10 M TBAP CH_2Cl_2 solution. For the Frumkin isotherms, values of *a* employed were 0.02, 0.03, and 0.04, respectively.

From the cyclic voltammograms, the surface coverages of the dendrimer-Fc_x were calculated by dividing the total coverage (from the coulometric charge) of ferrocene sites by the number of ferrocene sites within a single dendrimer molecule, assuming that all ferrocene sites were electrochemically active.

Parts A, B, and C of Figure 3 show the adsorption isotherms obtained in CH_2Cl_2 solutions of the dendrimers-Fc_{64}, -Fc_{32}, and -Fc_8, respectively. In order to determine which adsorption isotherm better described each data set, the values for Γ_s and β must be determined. Values of Γ_s and β for each dendrimer were obtained using a least-squares best fit of the experimental data to the parameters of the Langmuir equation (eq 2). The calculated values of Γ_s and β for the three dendrimers are summarized in Table 1. Values of Γ_s were in good accordance with theoretical ones (7.37×10^{-12}, 9.06×10^{-12}, and 2.45×10^{-11} mol cm^{-2}, respectively), which were calculated using diameters of 51, 46, and 28 Å for dendrimers-Fc_{64}, -Fc_{32}, and -Fc_8, respectively and assuming the adsorbed film has a hexagonal close-packed structure.

From the adsorption coefficient β, the adsorption free energy, $\Delta G°_{ads}$, was also determined, using

$$\Delta G°_{ads} = -RT \ln(55.5\beta) \qquad (4)$$

The calculated $\Delta G°_{ads}$ values are also summarized in Table 1. Although these dendrimers do not have groups with pendant adsorption sites, such as pyridyl, isocyanyl, or thiol groups, they nonetheless have relatively large adsorption free energies; similar to those of $[Os(bpy)_2ClL]^+$ (ca. −49 kJ mol^{-1}),[18] where bpy = 2,2′-bipyridine and L are various dipyridyl groups including 4,4′-bipyridine, *trans*-1,2-bis(4-pyridyl)ethylene, 1,3-bis(4-pyridyl)-propane, or 1,2-bis(4-pyridyl)ethane, all of which have a pendant pyridyl group through which adsorption takes place. However, Anson et al.[17] have recently shown that similar complexes with phenyl (rather than pyridine) pendant groups also adsorb, albeit not as strongly, suggesting the presence of significant van der Waals interactions. In the present case we believe that the adsorption is governed, at least in part, by surface/dendrimer as well as by van der Waals interactions likely due to the relatively large molecular weight of the dendrimers employed. The increase in $\Delta G°_{ads}$ with dendrimer size is consistent with this.

Based on the calculated values of Γ_s and β, the data for the dendrimers-Fc_{64}, -Fc_{32}, and -Fc_8 were fitted to the Langmuir isotherm (solid lines in Figure 3, parts A, B, and C, respectively). From a comparison of parts A, B, and C, it was clear that the saturation coverage of the dendrimers increased in the order $Fc_{64} < Fc_{32} < Fc_8$, as expected from the relative sizes of the dendrimers. The experimentally obtained coverages do not appear to have reached a saturation value over the concentration range examined. Measurements at higher solution concentration were complicated by the fact that there appears to be some degree of association of material in solution with the adsorbed monolayer, making coverage measurements under these conditions unreliable.

In Table 1, the calculated values of the interaction parameter, *a*, in the Frumkin equation (eq 3) are also listed. The values of *a* were calculated by best fitting the experimental data to the Frumkin isotherm, using the values of β obtained from fits to the Langmuir isotherm (solid lines in Figure 3), since the difference between the two isotherms is the degree of the adsorbate−adsorbate interaction. The broken lines in Figure 3A−C are best fits to the Frumkin isotherm using the *a* values listed in Table 1. The very small values of *a* obtained indicate that interactions between the adsorbed dendrimers are negligible. This appears reasonable since the dendrimers examined are uncharged at 0.0 V vs SSCE (reduced state), where adsorption was carried out. We have previously reported that adsorption of $[Os(bpy)_2ClL]^+$, which has a +1 charge in the reduced state, onto Pt electrodes was well-fitted to the Frumkin isotherm with $a = 0.2$.[18] An increase in the repulsive forces (i.e. increase in *a*) would be expected upon oxidation of the dendrimers to +1 charge. Unfortunately, since oxidation of the dendrimers examined gave rise to the rapid formation of a salt with the anion (see below), this was not examined further. However, from the above results, it can be stated that the adsorption of the dendrimers is well-described by the Langmuir isotherm.

(17) Campbell, John. L. E.; Anson, F. C. *Langmuir* **1996**, *12*, 4008.
(18) Acevedo, D.; Bretz, R. L.; Tirado, J. D.; Abruña, H. D. *Langmuir* **1994**, *10*, 1300.

Table 1. Values of Γ_s, β, $\Delta G°_{ads}$, and a for Dendrimer-Fc_{64}, -Fc_{32}, and -Fc_8 Deposited at 0.0 V vs SSCE in a 0.1 M TBAP CH_2Cl_2 Solution

	dendrimer-Fc_{64}	dendrimer-Fc_{32}	dendrimer-Fc_8
Γ_s (mol cm^{-2})	$(6.5 \pm 1.1) \times 10^{-12}$	$(1.4 \pm 0.2) \times 10^{-11}$	$(3.5 \pm 0.4) \times 10^{-11}$
β (L mol^{-1})	$(4.2 \pm 2.5) \times 10^{7}$	$(1.2 \pm 0.5) \times 10^{7}$	$(3.7 \pm 1.0) \times 10^{6}$
$\Delta G°_{ads}$ (kJ mol^{-1})	-53 ± 2	-50 ± 1	-47 ± 1
a	0.02	0.03	0.04

B. Kinetics. Next, we investigated the kinetics of adsorption. There are two general models that can be used to explain the kinetics of adsorption of the dendrimers under study, assuming an adsorption equilibrium. The first model involves kinetic (activation) control of the system,[19] whereas the other involves fast adsorption with mass transport or diffusion control, as derived by Reinmuth.[20] The detailed theory of these models especially with regards to redox-active self-assembling monolayers has been previously described.[14b] Briefly, the kinetic control model under Langmuirian adsorption conditions can be expressed as

$$\Gamma_t = \Gamma_e(1 - \exp(-k'C^*t)) \tag{5}$$

where Γ_t is the surface coverage of the adsorbate at time t, Γ_e is the equilibrium surface concentration at a given bulk concentration, and k' is the rate constant which contains the activity coefficient of $A_{(sol)}$. In this equation, as the bulk concentration C^* increases, the equilibrium surface coverage, Γ_e, will increase until the saturation value, Γ_s, is reached. Therefore until this concentration is reached, Γ_e, will be controlled by the bulk concentration.

The second model, i.e. the fast adsorption with mass transport or diffusion control model, assumes semiinfinite linear diffusion of a species in solution to a stationary plane with Langmuirian adsorption at the boundary, and it can be expressed as

$$\frac{\Gamma_c}{\Gamma_s} = K\left(\frac{C^*}{\Gamma_s}\right)(D_t)^{1/2} \tag{6}$$

where D is the diffusion coefficient of the adsorbate, $A_{(sol)}$, and K is a constant equal to $\pi^{-1/2}$.

In the present case we studied which model better described the adsorption kinetics of the dendrimers employed. If the adsorption behavior of the dendrimers obeys eq 5, it would mean that the system is under activation control, whereas if it obeys eq 6, it would mean that the adsorption kinetics is fast and the rate-limiting step is the diffusion of the adsorbate to the surface of the electrode.

Parts A, B, and C of Figure 4 show the time-dependence of the surface coverage at different solution concentrations for the dendrimers-Fc_{64}, -Fc_{32}, and -Fc_8, respectively. All the curves in the figures were obtained by fitting the data to eq 5 with Γ_e and k' as the adjustable parameters. As can be seen for all the dendrimers at virtually all concentrations examined, calculated curves are in good accordance with experimental data. On the other hand, attempts to fit the data to eq 6 with Γ_t and K as adjustable parameters gave rise to much larger deviations from the experimental data than those for fits to eq 5. Thus, these results indicate that the kinetics of adsorption of the dendrimer-Fc_x is well described by the activation control model. We also investigated the effect of the concentration of the adsorbates on the kinetics of adsorption. Table 2 lists the rate constants, k', calculated using best fitting of the data to the activation control equation (eq 5). As can be seen in Table 2, if the values at the lower concentrations, in which there exists a large experimental error due to the small volume injected, are neglected, the values of the kinetic parameters increase in the order $Fc_8 < Fc_{32} < Fc_{64}$, for dendrimer concentrations in the same range. For each dendrimer, the rate constant appears to be largely independent (with some exceptions) of concentration over the ranges of concentration examined. Thus, it appears that the adsorption kinetics are dependent

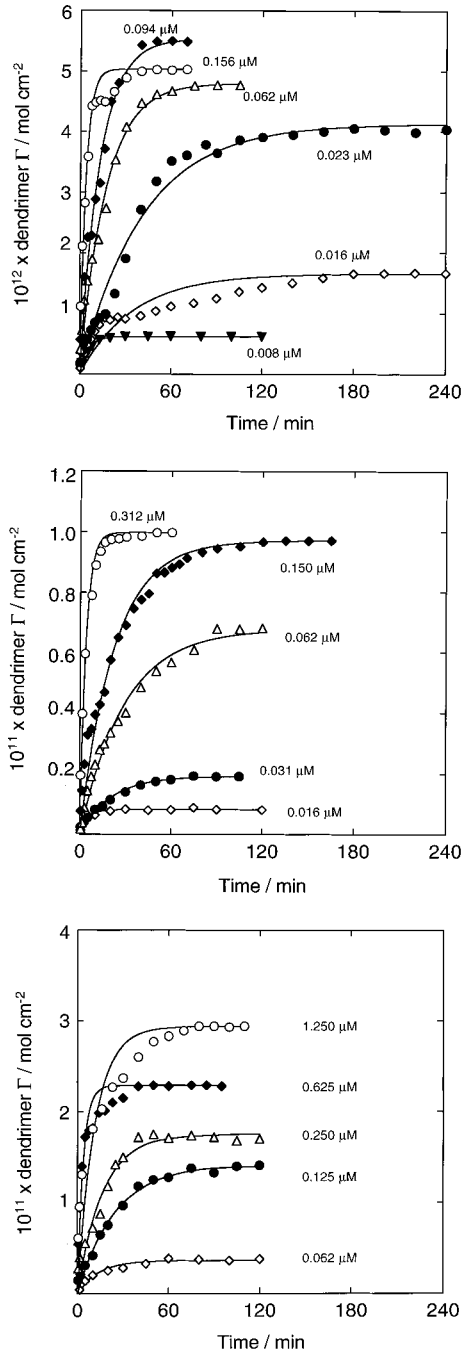

Figure 4. Adsorption kinetics at various concentrations of (A) dendrimer-Fc_{64}, (B) dendrimer-Fc_{32}, and (C) dendrimer-Fc_8 on a Pt electrode in a 0.10 M TBAP CH_2Cl_2 solution at 0.0 V vs SSCE.

(19) Parsons, R. In *Advances in Electrochemistry*; Delahay, P. Ed.; Interscience: New York, 1961; Vol. 1.

(20) Reinmuth, W. H. *J. Phys. Chem.* **1961**, *65*, 473.

Table 2. Kinetic Parameter for the Dendrimer-Fc_{64}, -Fc_{32}, and -Fc_8 Adsorbed at 0.0 V in a 0.1 M TBAP Ch_2Cl_2 Solution

dendrimer-Fc_{64}		dendrimer-Fc_{32}		dendrimer-Fc_8	
concn (μM)	k' (M^{-1} s^{-1})	concn (μM)	k' (M^{-1} s^{-1})	concn (μM)	k' (M^{-1} s^{-1})
0.156	$(3.0 \pm 0.3) \times 10^4$	0.312	$(1.4 \pm 0.1) \times 10^4$	1.250	$(1.2 \pm 0.2) \times 10^3$
0.094	$(1.4 \pm 0.1) \times 10^4$	0.250	$(1.1 \pm 0.1) \times 10^4$	0.625	$(7.1 \pm 0.8) \times 10^3$
0.062	$(1.6 \pm 0.1) \times 10^4$	0.150	$(5.0 \pm 0.2) \times 10^3$	0.250	$(4.1 \pm 0.4) \times 10^3$
0.031	$(1.2 \pm 0.2) \times 10^4$	0.062	$(9.2 \pm 0.6) \times 10^3$	0.186	$(4.1 \pm 0.3) \times 10^3$
0.023	$(1.7 \pm 0.1) \times 10^4$	0.047	$(8.3 \pm 0.4) \times 10^3$	0.125	$(5.4 \pm 0.4) \times 10^3$
0.016	$(3.0^a \pm 0.3) \times 10^4$	0.039	$(1.4^a \pm 0.2) \times 10^4$	0.094	$(2.4^a \pm 0.4) \times 10^4$
0.008	$(4.0^a \pm 0.2) \times 10^5$	0.031	$(2.6^a \pm 0.3) \times 10^4$	0.062	$(1.9^a \pm 0.3) \times 10^4$

[a] Not reliable.

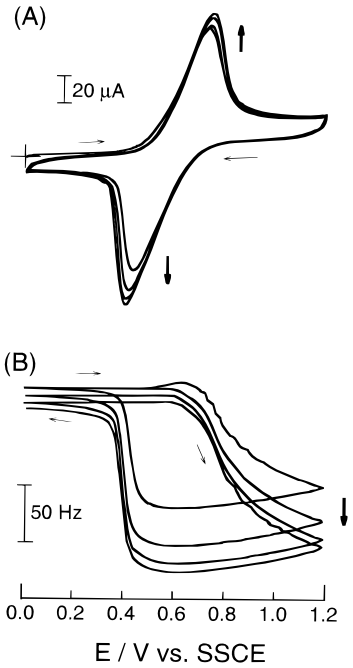

Figure 5. Typical (A) cyclic voltammogram (at 20 mV s^{-1}) and (B) frequency−potential curve for a Pt electrode in contact with a 15.6 μM dendrimer-Fc_{32} in a 0.10 M TBAP CH_2Cl_2 solution.

upon the identity of the dendrimer, but largely independent of concentration.

2. EQCM Studies: A. Electrodeposition Process in EQCM. We have also studied the electrodeposition processes of the dendrimers. In order to study the mass transfer during the electroadsorption of the dendrimers, changes in frequency due to the adsorption of the dendrimer-Fc_x onto a quartz crystal resonator were monitored while scanning the applied potential. The use of the EQCM is especially valuable for these studies since it allows for a separation of mass and electron transfer processes from changes in the resonant frequency as a function of applied potential with the concomitant measurement of current. In these experiments, a 0.5 mM solution concentration of ferrocenyl moieties was used, which corresponded to 7.81, 15.6, 31.2, and 62.5 μM solutions for the dendrimers-Fc_{64}, -Fc_{32}, -Fc_{16}, and -Fc_8, respectively. This relatively high concentration was chosen to obtain larger frequency changes for the EQCM experiments.

Figure 5 shows (A) the typical current (cyclic voltammogram) and (B) frequency responses as a function of applied potential for a Pt electrode in contact with a 0.10 M TBAP CH_2Cl_2 solution containing 15.6 μM dendrimer-Fc_{32}. Similar cyclic voltammograms and frequency−potential curves were obtained for dendrimer-Fc_8, -Fc_{16}, and -Fc_{64}. It should be noted that anodic waves showed a typical diffusional shape, whereas cathodic waves showed a stripping shape, indicating that the dendrimers adsorb onto the electrode during oxidation and desorb during reduction in a manner analogous to poly(vinylferrocene). The frequency responses obtained concurrently with the cyclic voltammograms also support these observations. As can be clearly ascertained in Figure 5, the frequency decreased during the anodic scan from +0.60 V vs SSCE, which is just prior to the anodic peak potential, to +1.20 V, where the sweep direction was reversed. The frequency continued to decrease gradually during the cathodic scan up to +0.60 V, and then it increased sharply from +0.42 to +0.38 V and reached an approximate steady state for the remainder the cathodic scan. Upon continued scanning there was a gradual and continuous shift in the frequency to lower values as can be clearly ascertained in Figure 5B. However, if the potential was held at 0.0 V, where the dendrimer is in its reduced form, there was a partial recovery, so the frequency gradually increased until it reached a steady state value that was several hertz lower than the initial one prior to adsorption of the dendrimer.

This suggests that in the oxidized form, the dendrimer appears to accumulate on the surface of the electrode (likely as a salt; vide infra). However upon reduction to the neutral form at 0.0 V, this material appears to gradually desorb so that only the strongly adsorbed material (presumably the first monolayer) remains on the surface of the electrode.

Decreases and increases in frequency are usually ascribed to mass loading and unloading, respectively, onto a quartz crystal resonator.[21] However, since changes in frequency are caused not only by changes in mass but also by changes in solution properties (such as viscosity and density),[22−24] film properties (such as viscoelasticity,[25,26] roughness,[27−29] and thickness),[31−33] and solvophilicity of the film in contact with the quartz crystal resonator, these frequency changes caused by the electrodeposition of the dendrimers onto the quartz crystal resonator need to be confirmed. In order to check for changes in these properties, admittance measurements of the quartz crystal resonator were carried out using an impedance analyzer, from which the resistance parameter of the electrical equivalent circuit for the quartz crystal resonator was evaluated. Since the resistance parameter, which is given as the reciprocal of the

(21) Sauerbrey, G. *Z. Phys.* **1959**, *155*, 206.
(22) Kanazawa, K. K.; Gordon, J. G., II *Anal. Chim. Acta* **1985**, *175*, 99.
(23) Muramatsu, H.; Tamiya, E.; Karube, I. *Anal. Chem.* **1988**, *60*, 2142.
(24) Martin, S. J.; Granstaff, V. E.; Frye, G. C. *Anal. Chem.* **1991**, *63*, 2272.
(25) Borjas, R.; Buttry, D. A. *J. Electroanal. Chem.* **1990**, *280*, 73.
(26) Muramatsu, H.; Ye, X.; Suda, M.; Sakuhara, T.; Ataka, T. *J. Electroanal. Chem.* **1992**, *332*, 311.
(27) Beck, R.; Pittermann, U.; Weil, K. G. *J. Electorochem. Soc.* **1992**, *139*, 453.
(28) Yang, M.; Thompson, M.; Duncan-Hawitt, W. C. *Langmuir* **1993**, *9*, 802.
(29) Yang, M.; Thompson, M. *Langmuir* **1993**, *9*, 1990.
(30) Bruckenstein, S.; Fensore, A.; Li, Z.; Hillman, A. R. *J. Electroanal. Chem.* **1994**, *370*, 189.
(31) Buttry, D. A.; Ward, M. D. *Chem. Rev.* **1992**, *92*, 1355.
(32) Okajima, T.; Sakurai, H.; Oyama, N.; Tokuda, K.; Ohsaka, T. *Electochim. Acta* **1993**, *38*, 747.
(33) Takada, K.; Tatsuma, T.; Oyama, N. *J. Chem. Soc., Faraday Trans.* **1995**, *91*, 1547.

maximum conductance for an ideal system, corresponds to a loss of mechanical energy dissipated to the surrounding medium, changes in the film properties will result in changes in the resistance parameter.[25,31,33−35] Thus, an increase in the resistance parameter indicates an increase in the viscoelasticity, roughness, and solvophilicity of the film on a quartz crystal resonator, whereas a decrease in the resistance parameter indicates a decrease in these properties.

Curves A, B, C, and D in Figure 6 show the time courses of the resistance parameter of the resonator in a 0.10 M TBAP CH_2Cl_2 solution each containing 0.5 mM ferrocenyl moieties of dendrimers-Fc_{64}, -Fc_{32}, -Fc_{16}, and -Fc_8, respectively, upon potential steps from the reduced (0.0 V vs SSCE) to the oxidized (+1.10 V) and back to the reduced (0.0 V) states of the ferrocenyl moieties of the dendrimers. For the dendrimer-Fc_{64}, the resistance parameter was found to increase sharply by ca. 40 Ω just after the anodic potential step (Figure 6A). This was followed by a further continuous increase of ca. 80 Ω during the time period examined (15 min). There was a sharp decrease of ca. 50 Ω just after the subsequent cathodic potential step. This was followed by a transient response where the resistance parameter initially increased (ca. 50 Ω) and subsequently decreased (ca. 60 Ω) to reach a steady state value within 15 min. A qualitatively similar behavior was found for the dendrimer-Fc_{32} (Figure 6B). In this case the resistance parameter increased sharply by ca. 35 Ω just after the anodic potential step, followed by a further increase (ca. 60 Ω) until the potential was stepped back to 0.0 V. The resistance parameter decreased sharply by ca. 65 Ω just after the cathodic potential step, followed by a large increase (ca. 85 Ω) and a subsequent decrease (ca. 90 Ω), before reaching a steady state. The behavior of dendrimer-Fc_8, however (Figure 6D), was quite different from those of dendrimers-Fc_{64} and -Fc_{32}. In this case the resistance parameter simply increased (no abrupt change) by ca. 190 Ω following the anodic potential step during the time range examined (15 min). Following the potential step to 0.0 V, it rapidly returned to its original value and attained a steady state within 10 min. Moreover, dendrimer-Fc_8 did not exhibit the transient behavior observed for dendrimers-Fc_{64} and -Fc_{32}. The behavior for dendrimers-Fc_{16} (Figure 6C) was intermediate between that exhibited by dendrimers-Fc_{64} (as well as -Fc_{32}) and -Fc_8. In this case the resistance parameter increased by ca. 20 Ω just after the anodic potential step, followed by a further increase (ca. 150 Ω) until the potential was stepped back to 0.0 V. The resistance parameter decreased somewhat sharply by ca. 40 Ω just after the cathodic potential step and then decreased monotonically without the transient feature observed for dendrimers-Fc_{64} and -Fc_{32}.

The increase in the resistance parameter upon oxidation (potential step to +1.10 V) for all dendrimers within the time period examined is believed to arise from a continuous increase in the thickness, roughness, and viscoelasticity of the film due to the continuous deposition of the dendrimer. In addition, the sudden increase in the resistance parameter just after the anodic potential step for dendrimers-Fc_{64} and -Fc_{32} and to a certain extent for dendrimers-Fc_{16} may reflect an abrupt deposition of the dendrimers. In the case of dendrimer-Fc_8, however, such an initial large increase in the resistance parameter was not observed. This suggests that oxidation of dendrimer-Fc_8 does not give rise to an abrupt change in film properties with deposition, probably resulting from the relatively smaller size of dendrimer-Fc_8 compared to those of the other dendrimers, especially dendrimers-Fc_{64} and -Fc_{32}, which makes the film better packed, i.e. more rigid. As mentioned above, the diameters of the dendrimers-Fc_8, -Fc_{16}, -Fc_{32}, and -Fc_{64} are estimated to be 28, 38, 46, and 51 Å, respectively. The initial

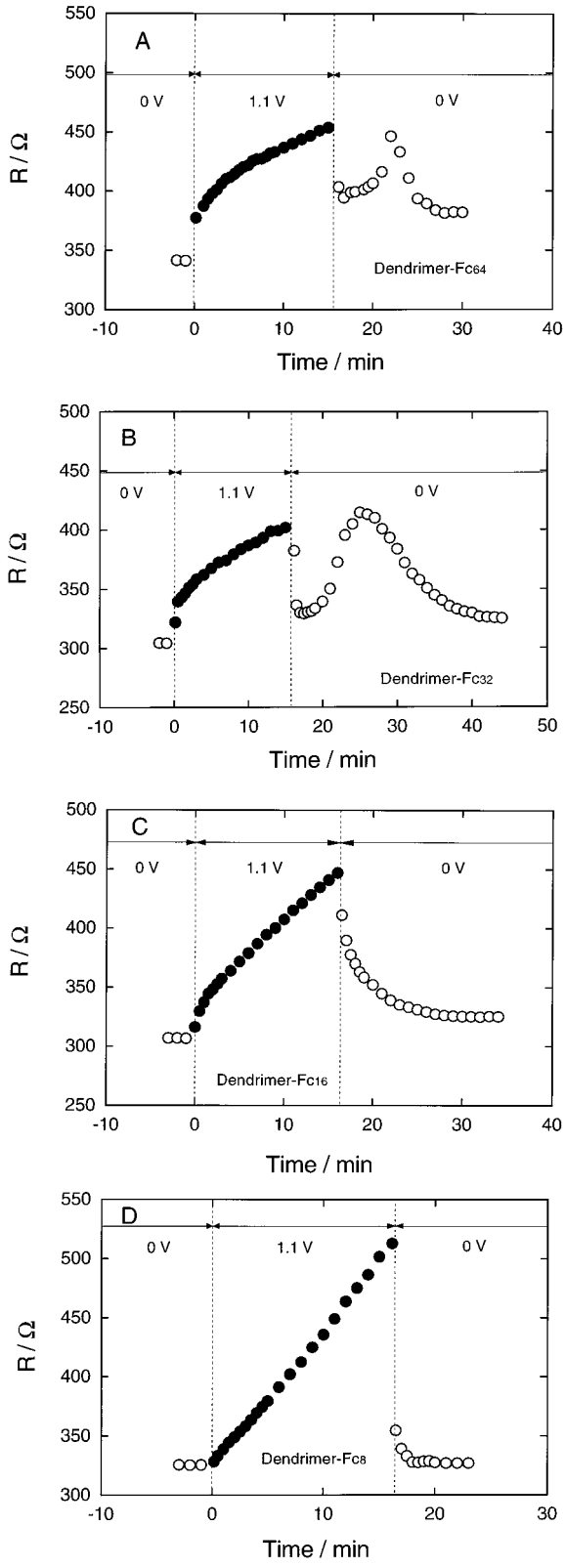

Figure 6. Time courses of the resistance parameter of a quartz crystal resonator during potential step experiments (between 0.0 V and +1.10 V vs SSCE) in a 0.10 M TBAP AN solution containing 0.5 mM ferrocenyl moieties of (A) dendrimer-Fc_{64}, (B) dendrimer-Fc_{32}, (C) dendrimer-Fc_{16}, and (D) dendrimer-Fc_8.

(34) Oyama, N.; Tatsuma, T.; Takahashi, K. *J. Phys. Chem.* **1993**, *97*, 10504.
(35) Tatsuma, T.; Takada, K.; Matsui, H.; Oyama, N. *Macromolecules* **1994**, *27*, 6687.

abrupt decrease in the resistance parameter for all dendrimers just after the cathodic potential step may arise from the dissolution of electrodeposited dendrimers. The transient changes in the resistance parameter observed for dendrimers-Fc_{64} and -Fc_{32} after sharp decreases upon reduction may be caused by a temporary increase in the roughness or other properties of the film. From these results it appears that the oxidized form of the dendrimers deposits onto the Pt electrode, while the reduced form is easily redissolved. In addition, deposition and dissolution processes appear to give rise to large changes in the film properties of the dendrimers. Unfortunately, these results indicate that it is difficult to unambiguously calculate the changes in the mass of the dendrimers during the deposition and dissolution processes in a 0.10 M TBAP CH_2Cl_2 solution from changes in the frequency measured by EQCM, as mentioned above.

We have additional EQCM evidence of the deposition of the dendrimer upon oxidation onto a Pt electrode. When the potential was scanned to a less positive limit (+0.90 V vs SSCE) relative to that for curves A and B in Figure 5 (up to +1.20 V), the oxidative peak current of the voltammogram of dendrimer-Fc_{32} was almost the same, whereas the reduction current peak height was smaller by about 15 μA. In addition, the frequency-potential curve obtained when the potential was scanned up +0.90 V showed a smaller frequency decrease upon oxidation and a smaller increase upon reduction relative to those in curve B in Figure 5. Similar results were obtained for dendrimers-Fc_{64}, -Fc_{16}, and -Fc_8. These results indicate that as long as the applied potential lies positive of the redox potential of the dendrimers, the oxidized dendrimer-Fc_x is continuously deposited onto the electrode and is subsequently redissolved into the solution upon reduction.

From these results it appears that the dendrimers-Fc_x are electrodeposited onto Pt electrodes upon oxidation, likely due to the low solubility of the salt derived from the oxidized dendrimer and ClO_4^- anions. Upon reduction, the material is redissolved except for the strongly adsorbed dendrimers, which ostensibly make the first monolayer.

B. Mass Transfer Process of Electrodes Modified with Dendrimers-Fc_x. We now consider the mass transport process accompanying the redox transformations of the surface immobilized dendrimers. In order to carry out such studies, changes in the frequency of the dendrimer-Fc_x adsorbed onto the quartz crystal resonator were monitored while scanning the applied potential. These measurements were carried out just after the electrodeposition experiments, as mentioned in the previous section. Figure 7 shows (A) the typical current (cyclic voltammogram) and (B) frequency responses of the dendrimer-Fc_{32} deposited onto a Pt electrode as a function of applied potential between +0.20 and +0.90 V vs SSCE in a 0.10 M TBAP AN solution. Similar cyclic voltammograms and frequency responses were obtained for electrodes modified with dendrimers-Fc_{64}, -Fc_{16}, and -Fc_8. The changes in frequency, which are defined as the difference between the maximum and minimum frequencies in the reduced and oxidized states during several potential scans at various scan rates, are summarized in Table 3. Over the scan rate range examined, the peak current in the cyclic voltammogram was directly proportional to scan rate as anticipated for a surface immobilized reagent.

As described earlier, since the frequency of the quartz crystal resonator is sensitive not only to mass changes but also to the rigidity, roughness, and solvophilicity of the film surface, it is important to establish the main factor(s) giving rise to the frequency changes during the redox reaction of the adsorbed layer on the quartz crystal resonator. Admittance measurements

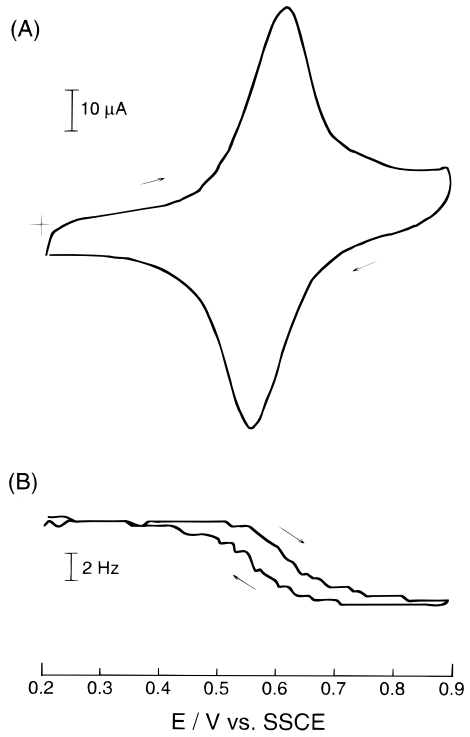

Figure 7. Typical (A) cyclic voltammogram (at 50 mV s^{-1}) and (B) frequency-potential curve of the dendrimer-Fc_{32} adsorbed onto a quartz crystal resonator in a 0.10 M TBAP AN solution.

of the quartz crystal resonator were carried out, and the maximum difference observed in the resistance parameter for the dendrimers adsorbed onto the quartz crystal resonator in a 0.10 M TBAP AN solution between the oxidized (+1.10 V vs SSCE) and reduced (0.0 V) states was 2.0 Ω. This result demonstrates that the main factor giving rise to the frequency changes during redox transformations is the change in the mass of the dendrimer-Fc_x film, in order to maintain the electroneutrality of the film. Therefore, changes in mass can be estimated from the changes in the frequency of the quartz crystal resonator using the Sauerbrey equation[21]

$$\Delta m = -C_f \Delta f \tag{7}$$

where Δm (g cm^{-2}) is the total change in mass, C_f (g Hz^{-1} cm^{-2}) is a proportionality constant for an AT-cut quartz crystal resonator, and Δf (Hz) is the change in frequency. Here, we used a value of 17.7×10^{-9} g Hz^{-1} cm^{-2} for C_f.

As can be seen in Figure 7, the oxidation reaction causes a decrease in the frequency, corresponding to an increase in the mass of the adsorbed dendrimer film, while the reduction reaction causes an increase in the frequency, corresponding to a decrease in the mass of the film. These changes in frequency can be considered as a manifestation of anion and/or solvent (AN) incorporation upon oxidation, and ejection upon reduction across the film/solution interface, because the oxidized and reduced ferrocenyl sites have net +1 and 0 charges, respectively.

The mass transfer equivalent, M_{eq} (g mol^{-1}), which gives an indication of the change in mass per ferrocenyl site of the adsorbed dendrimer molecule during the redox reaction, was calculated by dividing the change in mass (g cm^{-2}) caused by the movement of ClO_4^- anions and/or AN by the surface coverage of the ferrocenyl sites of the adsorbed dendrimers, Γ_{Fc} (mol cm^{-2}). Calculated M_{eq} values for the dendrimers-Fc_{64}, -Fc_{32}, -Fc_{16}, and -Fc_8 in a 0.10 M TBAP AN solutions are also summarized in Table 3.

Table 3. Mass-Charge Correlations of the Dendrimer-Fc_{64}, -Fc_{32}, and -Fc_8-Modified Electrode in a 0.1 M TBAP AN Solution

	scan rate ($mV\ s^{-1}$)	ΔF (Hz)	Γ_{Fc} ($mol\ cm^{-2}$)	Γ_{dend} ($mol\ cm^{-2}$)	M_{eq} ($g\ mol^{-1}$)	no. of AN molecules/-Fc site + ClO_4^-
Dendrimer-Fc_{64}	50	−9.8	5.6×10^{-10}	8.8×10^{-12}	307.1	5.1
	20	−11.1	5.6×10^{-10}	8.8×10^{-12}	347.7	6.0
	10	−11.6	5.6×10^{-10}	8.8×10^{-12}	363.5	6.4
Dendrimer-Fc_{32}	50	−6.9	9.8×10^{-10}	3.1×10^{-11}	124.0	0.6
	20	−6.7	9.8×10^{-10}	3.1×10^{-11}	120.0	0.5
	10	−4.8	9.8×10^{-10}	3.1×10^{-11}	81.8	−0.3
Dendrimer-Fc_{16}	50	−8.0	1.1×10^{-9}	7.0×10^{-11}	126.3	0.6
	20	−6.8	1.1×10^{-9}	7.0×10^{-11}	107.4	0.2
	10	−6.8	1.1×10^{-9}	7.0×10^{-11}	107.4	0.2
Dendrimer-Fc_8	50	−6.7	6.9×10^{-10}	8.6×10^{-11}	171.9	1.8
	20	−6.7	6.9×10^{-10}	8.6×10^{-11}	171.9	1.8
	10	−5.1	6.9×10^{-10}	8.6×10^{-11}	130.4	0.7

It should be noted that although these dendrimer films were electrodeposited and prepared from higher concentration solutions (0.5 mM ferrocenyl site) compared to those of the experiments in the adsorption process section (0.5−10 μM ferrocenyl site), the coverages of the dendrimers (not ferrocenyl sites) obtained, and shown in Table 3, were in good accordance with theoretical coverages, assuming that the films have a hexagonal close-packed structure, as described above. This suggests that of all the dendrimers examined gave rise to the adsorption of only one monolayer on the Pt electrode surface at ferrocenyl concentrations above ca. 10 μM (even at 0.5 mM), as long as the dendrimers were in the reduced form. This again suggests that in the reduced form the interactions between dendrimers is weak and that the use of the Langmuir isotherm to describe the thermodynamics of adsorption under these conditions is appropriate, as described earlier.

In terms of the value of M_{eq}, if only the anion moves across the interface between the dendrimer film and the solution, then values of 99 would be expected for TBAP solutions. Values of M_{eq} in excess of 99 would be due to the movement of solvent (AN) molecules accompanying the exchanging anions. The calculated numbers of solvent (AN) molecules exchanged are also listed in Table 3. As shown in Table 3, it is estimated that ca. 5−6.5, 0−1, 0.2−0.6, and 0.5−2 solvent molecules per redox site move with the ClO_4^- anion for dendrimers-Fc_{64}, -Fc_{32}, -Fc_{16}, and -Fc_8, respectively. In addition, these values were independent of scan rate. Although this is clearly a limited set of data, some remarks might be appropriate. First of all, the number of solvent molecules per anion exchanged is much larger for dendrimer-Fc_{64} than for all the other dendrimers, suggesting large changes in solvation accompanying the redox reaction for this material. For the other dendrimers, dendrimer-Fc_8 exhibits the second largest change, with dendrimers-Fc_{32} and -Fc_{16} exhibiting similar and much smaller changes. These changes in solvation follow, in a qualitative sense, variations in charge density (calculated from the size of the dendrimers and the number of ferrocene units per molecule), which suggests that this might be responsible, at least in part, for the observed behavior.

Hillman et al.[36] have reported that for electrodes modified with redox-active films, the reorganization of the film structure upon the redox reaction may include three processes. In the first, the redox process is accompanied by the movement of charged particles to maintain electroneutrality within the film. This process may be followed by assimilation and expulsion of noncharged solvent to achieve a state of solvation within the film that is appropriate for the resulting charge distribution. Finally, the film may undergo segmental motion to adopt a new morphology. A qualitatively similar situation may be operative in the present case; in particular, changes in the extent of solvation with oxidation state as well as the transient behavior observed in the impedance experiments upon stepping the potential from +1.10 V where the dendrimers are in the oxidized form to 0.0 V where they are in the reduced form. It is also likely that there are structural changes that accompany the redox transformations.

(36) Hillman, A. R.; Hughes, N. A.; Bruckenstein, S. *Analyst* **1994**, *119*, 167.

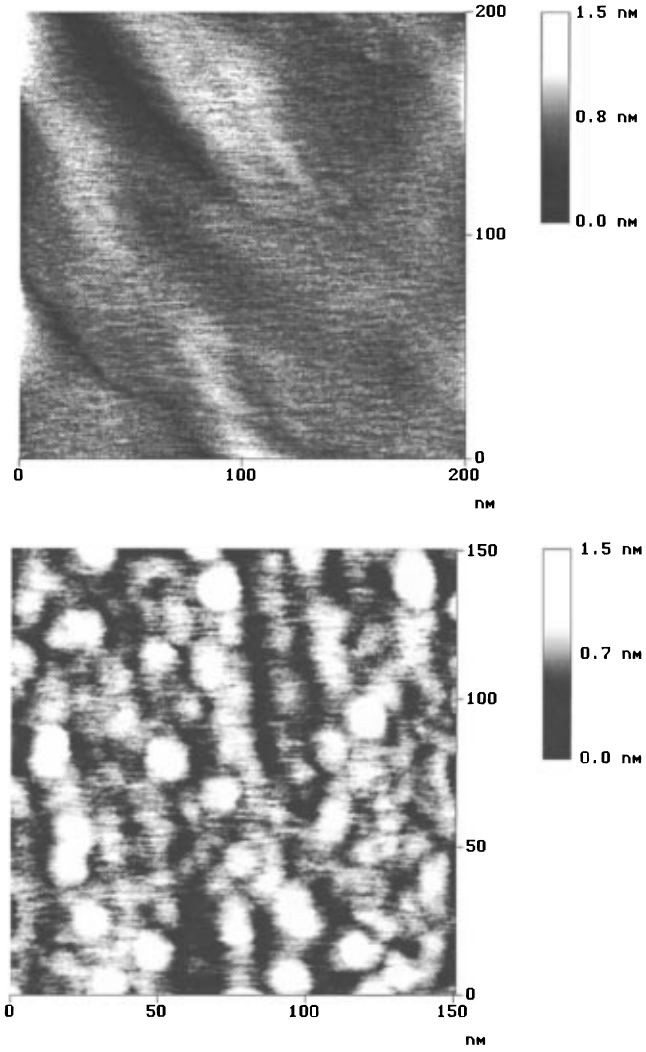

Figure 8. (A) 200 nm × 200 nm TMAFM image of a freshly annealed Pt(111) single crystal surface and (B) 150 nm x 150 nm TMAFM image of a dendrimer-Fc_{64}-modified Pt(111) single crystal surface surface.

3. Tapping Mode AFM Imaging of Dendrimer-Fc_{64} Adsorbed onto a Pt(111) Single Crystal Electrode. We have also carried out preliminary TMAFM imaging studies of

dendrimer-Fc_{64} adsorbed onto a Pt(111) single crystal electrode. Figure 8A, B shows the imaging of the platinum surface prior to and after modification with dendrimer-Fc_{64}. Prior to modification, the surface appears essentially smooth and featureless. However, upon modification there is clear evidence of the presence of adsorbed dendrimer-Fc_{64}. The circular features that can be seen over the entire image represent individual dendrimer units. Also from the figure, it is evident that in some cases there appear to be aggregates present on the surface. We ascribe these brighter spots to the presence of adsorbates that are two dendrimer units in height and which likely result from the evaporation of the CH_2Cl_2 solvent. A preliminary analysis of these images suggests that the apparent size of the adsorbed dendrimer is significantly larger than the calculated (51 Å diameter) value. We believe that this is due, in part, to a convolution of the tip profile and the sample as well as to a flattening of the dendrimer upon adsorption. Flattening of dendrimers upon adsorption has been has been previously predicted by Mansfield[37] using Monte Carlo simulations where the analysis was based on the generation number (G) of the dendrimer and the interaction strength (A) of the dendrimer with the surface. Such behavior upon adsorption has also been suggested by Crooks and co-worker[38] and recently experimentally observed by Sheiko and co-workers,[39] using scanning force microscopy, and Tsukruk and co-workers,[40] who employed scanned probe microscopy and X-ray reflectivity. However, in none of these cases were molecularly resolved images presented.

We are currently carrying out additional studies of this as well as the other dendrimers including in-situ measurements with the intent of determining the surface structures of these adsorbed dendrimers as well as changes with the applied potential with particular interest in comparing and contrasting images at potentials where the ferrocenyl groups within the dendrimers are in the oxidized or reduced forms.

(37) Mansfield, M. L. *Polymer* **1996**, *37*, 3835.
(38) Wells, M.; Crooks, R. M. *J. Am. Chem. Soc*. **1996**, *118*, 3988.
(39) Sheiko, S. S.; Eckert, G.; Ignat'eva, G.; Muzafarov, A. M.; Spickermann, J.; Räder, H. J.; Möller, M. *Macromol. Rapid Commun.* **1996**, *17*, 283.
(40) Tsukruk, V. V.; Rinderspacher, F.; Bliznyuk, V. N. *Langmuir* **1997**, *13*, 2171.

Conclusions

The adsorption thermodynamics and kinetics of ferrocenyl containing dendrimers onto a Pt electrode have been studied. The adsorption thermodynamics of the reduced form of the dendrimers in a CH_2Cl_2 solution is well represented by the Langmuir adsorption isotherm. The surface coverage of these dendrimers increased in the order $Fc_{64} < Fc_{32} < Fc_8$, which suggests that this is likely controlled by their molecular sizes. The adsorption free energies, $\Delta G°_{ads}$, for dendrimers-Fc_{64}, -Fc_{32}, and -Fc_8 were found to be -53 ± 2, -50 ± 1, and -47 ± 1 kJ mol^{-1}, respectively. We attribute these differences in $\Delta G°_{ads}$ values to a decrease in van der Waals interactions. The kinetics of adsorption appears to be activation-controlled rather than diffusion-controlled and to be dependent upon the identity of the dendrimer, but independent of concentration.

With the EQCM technique and, in particular, from an analysis of admittance measurements of the resonator, it appears that the oxidized form of the dendrimers deposits onto the Pt electrode, likely due to low solubility of the salt of oxidized dendrimer (ferricenium form) and ClO_4^- anions, whereas the reduced form of the dendrimers easily redissolves except for the first monolayer, which appears to be strongly adsorbed. Further, the mass transfer process during the redox reaction of the adsorbed dendrimers in an AN solution was found to be of the anion exchange type. In addition, it was determined that the ClO_4^- anions are accompanied by AN molecules, whose numbers appear to depend on the charge density (density of ferrocenyl groups) of each dendrimer. Additionally, admittance measurements of the resonator established that no film property changes occur during the redox reaction of the adsorbed dendrimers.

Imaging by TMAFM of dendrimer-Fc_{64}, adsorbed onto a Pt surface, suggests that, upon adsorption, there is a flattening of the molecules.

Acknowledgment. This work was supported by the Office of Naval Research and the DGICyT of Spain (Project PB-93-0287). D.D. acknowledges support by a Sage Graduate Fellowship from Cornell University.

JA9716315